

Digital twin of Calais canal with model predictive controller: a simulation on real database

Roza Ranjbar¹, Pablo Segovia², Eric Duviella³, Lucien Etienne⁴, José M. Maestre⁵, and Eduardo F. Camacho⁶

¹Ph.D. Candidate, CERI Digital Systems, IMT Nord Europe, Lille, France (corresponding author). Email: `roza.ranjbar@imt-lille-douai.fr`

²Postdoctoral fellow, Dept. of Maritime and Transport Technology, Delft University of Technology, Delft, The Netherlands.

³Professor, CERI Digital Systems, IMT Nord Europe, Lille, France.

⁴Assistant professor, CERI Digital Systems, IMT Nord Europe, Lille, France.

⁵Professor, Dept. of Systems and Automation Engineering, University of Seville, Seville, Spain.

⁶Professor, Dept. of Systems and Automation Engineering, University of Seville, Seville, Spain.

Abstract

This paper presents the design of a Model Predictive Control (MPC) for the Calais canal, located in the north of France for satisfactory management of the system. To estimate the unknown inputs/outputs arising from the uncontrolled pumps, a Digital Twin (DT) in the framework of a Matlab-SIC² is used to reproduce the dynamics of the canal, and the real database corresponding to a period of three days is employed to evaluate the control strategy. The canal is characterized by two operating modes due to high and low tides. As a consequence of this, time-varying constraints on the use of gates must be considered, which leads to the design of two multi-objective control problems, one for the high tide and another for the low tide. Furthermore, a moving horizon estimation (MHE) strategy is used to provide the MPC with unmeasured states. The simulation results show that the different objectives are met satisfactorily.

Keywords: inland waterways; digital twin; model predictive control; real database; unknown inputs/outputs.

INTRODUCTION

Inland waterways are large and complex networked systems that supply various human needs such as water demand and the transportation of passengers and goods. They consist of multiple reaches and are usually connected to rivers, seas, lakes, and other waterways. Since the dynamics of these systems are naturally slow and characterized by transport delays, their management is challenging.

The key operational goal of inland waterway management is that of maintaining the available water at a specific level to meet various objectives, e.g., safe vessel navigation, avoiding natural hazards (such as floods), dealing with the impacts of climate change, and meeting irrigation and agricultural demands, to name a few (Vermuyten et al., 2018; Duviella et al., 2018). To do so, a set point known as the Normal Navigation Level (*NNL*) is defined for each reach, together with a navigation rectangle defining an admissible water level interval. This rectangle has a High Navigation Level (*HNL*) and a Low Navigation Level (*LNL*): when the water level is outside of the navigation rectangle, the navigation must stop (Segovia et al., 2018). Another important objective regarding the management of large-scale waterways is minimizing operational costs. Inland waterways are equipped with different hydraulic structures, e.g., gates and pumps, for water conveyance. Decisions regarding how and when to use the mentioned equipment have a direct impact on the operational costs (Puig et al., 2017). To deal with such challenging systems, advanced control techniques are essential to meet the objectives. Concerning water systems, model predictive control (MPC) has shown significant success in the operational management of water systems (Castelletti et al., 2023). MPC solves an online finite-horizon optimization problem at each sampling instant and determines optimal control actions ahead of time, of which only the first element is applied on the system. The next time, the procedure is repeated with updated system information, following a receding horizon policy (Maciejowski, 2002). MPC was employed by Fele et al. (2014) to find the optimal trade-off between control performance and communication costs

by modifying the network topology. [Zafra-Cabeza et al. \(2011\)](#) investigated a two-level MPC, with the top layer applying a risk management strategy and the lower layer solving distributed model predictive control problems for optimal performance. A multi-scenario MPC was employed by [Tian et al. \(2017\)](#) to control the North Sea Canal (the Netherlands) while analyzing its computational time. [Velarde et al. \(2019\)](#) investigated a scenario-based distributed MPC for water systems management with uncertainty. [Nasir et al. \(2019\)](#) developed a stochastic model predictive control to determine the reference inputs by using a model of the channel dynamics that includes a forecast of off-take demand and solving a chance-constraint optimization problem. The problem of handling drastic inflow fluctuations was studied by [Shahdany et al. \(2016\)](#) using a centralized model predictive controller.

There is always an extent of errors arising from a lack of data, e.g., hydraulic variables, in real case studies. This introduces a significant level of uncertainty in the values of the physical parameters used in the simulation, which might lead to inaccurate predictions. One appropriate approach to deal with these uncertainties consists in reproducing the dynamics of the network with a simulator. In this regard, the Digital Twin (DT) technique may be used to reproduce past events with an available calibrated model. In this way, one can determine the unknown inputs/outputs of a waterway system. For instance, by having real data on water levels and control signals during a period of time and a known initial condition, the water volume balance can be measured. Next, one can figure out the missing flows during the considered period of time. Finally, after estimating the unknown inputs/outputs, the past scenarios can be replayed, providing hindsight on the applied management policies ([Duviella and Hadid, 2019](#)). Several examples of applying digital twins over water system control can be found in the literature ([Conejos Fuertes et al., 2020](#); [Bartos and Kerkez, 2021](#); [Ramos et al., 2022](#); [Zekri et al., 2022](#); [Liu et al., 2023](#)). One important asset of DT is its direct connection to numerical computing environments, e.g., Matlab, to design the appropriate control strategy, which can then be tuned via DT. The work of [Ranjbar et al. \(2020\)](#) shows this approach by determining the difference of volume in the canal and averaging it on time so that the difference in discharges between two periods of time corresponds to the unknown inputs on the

canal.

The main contribution of this paper is the analysis of a real problem and a tailored solution for the Calais canal, which is affected by tides. This is different from what was done in Segovia et al. (2019), as it presented a general methodology for water level regulation in inland waterways. This work also uses a combination of MPC-MHE together with a DT to determine the missing inputs/outputs of the real database. Deshays et al. (2021) proposed an accurate DT with GIS data of the topography of a canal, leading to an error of less than 1 m. However, only a very simple control strategy based on logic rules was tested. This is probably due to the fact that the model featured a very large number of cross-sections, which would translate into an extensive number of states in a state-space representation. This fact prevents that model from being used as a prediction model in more complex control approaches, as it would increase the computation time required to determine the solution. For instance, if the DT model was employed as the internal model of a nonlinear MPC controller, the optimization function would have to execute the DT multiple times before generating a sequence of control actions. This can be highly restrictive, especially considering the timing constraints, even if the time required for each internal run of the DT is on the order of tens of seconds.

Segovia et al. (2020) and Karimi Pour et al. (2022) proposed similar control approaches wherein the main focus was to regulate the water levels and schedule the actuators. Although these works applied a different control strategy than Segovia et al. (2019) by employing a two-layer controller, one consisting of an MPC and the other for pump scheduling, these papers did not perform simulations on a real database of disturbances included in the canal. This paper proposes a solution to a multi-objective operational problem while handling physical and operational constraints, e.g., navigability, operating costs, and smooth control. Moreover, due to the lack of data from the real database in some geographical parts, a DT is designed by reproducing the behavior of the real system and missing information has been generated for a specific period of time, in an offline mode, and by rebuilding past scenarios and events such as periods of rainfalls, the managers are able to control the water levels in the canal regardless of the type of controller utilized, thereby eliminating the

need to exclusively rely on an MPC controller. In this context, the results of the advanced approach applied in this study are compared with manager-based control, which is based on the algorithm applied in [Duviella and Hadid \(2019\)](#) that uses regulation based on expert rules. The basis of these rules is described in section 5. Through this comparison, the benefits of utilizing real-world data will be illustrated for accuracy and the versatility of applying various control strategies.

The rest of the paper is organized as follows: Section 2 formalizes the problems for the water system. Section 3, illustrates the proposed framework. In Section 4, the case study is explained schematically, and Section 5 illustrates the benchmark against which the proposed control architecture will be compared in a later stage. Finally, Section 6 displays the potential of the proposed approach in a simulation of the case study, and the conclusions are presented in Section 7.

PROBLEM STATEMENT

Inland waterways are characterized by different elements, e.g., reaches, locks, gates, and nodes, the nature of which must be taken into account to satisfy the regulation objective. Inland waterway dynamics are typically modeled using the Shallow Water Equations (Saint-Venant equations), which are nonlinear partial differential equations that accurately describe the dynamics of open-flow systems ([Bresch, 2009](#)). However, due to their sensitivity to geometry and their non-linearity, they are not suited for real-time control. A solution to deal with such models is using one linear model, which is obtained by linearizing the original Saint-Venant equations around an operating point and assuming that the one operating point is adequate to characterize the system dynamics. Some examples of these models are the Integrator Delay (ID) model ([Schuurmans et al., 1999](#)), the Integrator Resonance (IR) model ([van Overloop et al., 2014](#)) and the Integrator Delay Zero (IDZ) model ([Litrico and Fromion, 2009](#)). Since the average flow in the case study of this work does not differ highly from the operating point, it is possible to consider a linear model and consequently choose one of the simplified models above-mentioned to link with the controller. Thus, here, the IDZ model is selected as it has proven adequate performance in the past ([Clemmens et al., 2017](#); [Segovia et al., 2019](#)). The IDZ input-output model links the discharges and the water levels at each

reach boundary and is given by

$$\begin{bmatrix} y_1(s) \\ y_2(s) \end{bmatrix} = \begin{bmatrix} p_{11}(s) & p_{12}(s) \\ p_{21}(s) & p_{22}(s) \end{bmatrix} \begin{bmatrix} q_1(s) \\ q_2(s) \end{bmatrix}, \quad (1)$$

where subscripts 1 and 2 refer to the upstream and downstream end of each reach, respectively, $y_1(s)$ and $y_2(s)$ denote the water levels and $q_1(s)$ and $q_2(s)$ are the reach inflow and outflow, in the corresponding order. Furthermore, $p_{ij}(s)$ are the IDZ terms

$$p_{ij}(s) = \frac{z_{ij}s + 1}{A_{ij}s} e^{-\tau_{ij}s}. \quad (2)$$

It can be seen that the IDZ model includes an integrator with a gain equal to $1/A_{ij}$, a time delay τ_{ij} and a zero equal to $-1/z_{ij}$, for $i, j = \{1, 2\}$. Then, the discrete-time linear state-space representation of the IDZ model can be formulated according to (Segovia et al., 2019) as follows:

$$\mathbf{x}_{k+1} = \begin{bmatrix} 1 & 0 \\ 0 & 1 \end{bmatrix} \mathbf{x}_k + \begin{bmatrix} T_s & 0 \\ 0 & -T_s \end{bmatrix} \mathbf{q}_k + \begin{bmatrix} 0 & -T_s \\ T_s & 0 \end{bmatrix} \mathbf{q}_{k-n}, \quad (3)$$

$$\mathbf{y}_k = \begin{bmatrix} \frac{1}{A_u} & 0 \\ 0 & \frac{1}{A_d} \end{bmatrix} \mathbf{x}_k + \begin{bmatrix} \frac{z_{11}}{A_u} & 0 \\ 0 & \frac{-z_{22}}{A_d} \end{bmatrix} \mathbf{q}_k + \begin{bmatrix} 0 & \frac{-z_{12}}{A_u} \\ \frac{z_{21}}{A_d} & 0 \end{bmatrix} \mathbf{q}_{k-n}. \quad (4)$$

In the state-space model formulation, $x_k \in \mathbb{R}^{n_x}$ denotes the water volumes, $q_k \in \mathbb{R}^{n_u}$ represents the water discharges by the actuators, q_{k-n} are the same delayed discharges (by n samples), and $y_k \in \mathbb{R}^{n_y}$ are the water levels. Moreover, A_u , A_d , z_{11} , z_{12} , z_{21} and z_{22} are the parameters of IDZ model, which are given in Litrico and Fromion (2009). Furthermore, T_s is the sampling time.

Keeping the water level close to the *NNL* is always a big concern for inland waterway managers due to the effects on transport and water supply. Weather changes such as periods of heavy rainfall usually impact water resources management. In this paper, canals are operated to convey the excess water to the sea. To this end, pumping stations and gates must be used. Moreover, sea tides should be considered due to their effect on scheduling the available actuators, as the downstream outlet

152 sea gates cannot be utilized during high tide periods for safety reasons. Thus, low/high operating
153 modes shall be defined for the control operation. Obviously, each operation entails a cost, and one
154 of the most important objectives in water systems management is minimizing the operational costs.
155 For instance, pumps should be used as a last resort as their operation is very costly, and only when
156 the situation requires it, e.g., avoiding spills and overflows. Therefore, the use of gravity gates is
157 preferable, even if this results in larger water level oscillations.

158 With all this in mind, the proposed solution consists of designing a multi-objective control
159 strategy for a multi-input multi-output system with complex dynamics subjected to physical con-
160 straints, affected by known and unknown disturbances. To this end, Model Predictive Control
161 (MPC) is chosen as the control approach due to its capability to optimize the future behavior of
162 the variables (Camacho and Bordons, 2007). Since the system states must be known, and due to
163 the fact that there are some immeasurable states, the use of an observer is required. Here, Moving
164 Horizon Estimation (MHE) is selected as the observer approach due to its ease of integration with
165 MPC, since it can also be formulated as an online optimization problem that deals with constraints.
166 Given a set of past input-output data, the solution of the MHE is a reconstructed sequence of state
167 estimates, and the last value of the sequence can be provided to the MPC to compute a new solution
168 at the next time instant using a receding horizon approach (Copp and Hespanha, 2017).

169 **PROPOSED APPROACH**

170 To ensure that a hydraulic model represents the real system precisely and accurately, model
171 results must be compared with the physical measurements over certain criteria. Upon the condition
172 that model prediction matches the data, the model is reliable to be used for the criteria that it
173 was calibrated for (Walski, 2017). Thus, most of the time, hydraulic models require calibrations
174 before being employed in control applications. In this case, different parameters of the system, e.g.,
175 topography, dimensions, slope, and roughness coefficients, are taken into account, and they should
176 be accurate to avoid major errors. Therefore, the values of these parameters have been refined until
177 the simulation architecture produces a solution that aligns with the data. Bearing the calibration
178 in mind, this approach has been proposed and validated using a combined simulation architecture

between Matlab and SIC² (Simulation and Integration of Control for Canals) software. Matlab will be used to compute the optimal control actions using a simplified prediction model. These actions will then be applied in the simulation model in SIC² to assess their impact on the system. The link between Matlab and SIC² will be discussed next.

Overall control architecture

Data from the canal, including water flows and levels, is collected, and control actions performed by managers are recorded. A subset of this data is selected and filtered to focus on specific time periods and relevant information. The filtered data is used as input for a designed digital twin (DT) working with Matlab-SIC² to estimate unknown flows. Once the DT provides this information by reproducing the real dynamics of the system, it can be regularly used at every time step of the simulation. This process is done offline. On the other hand, the water levels coming both from the filtered data and SIC² become a joint input for Matlab so that the control actions are determined and sent once again to SIC².

These steps are repeated every time instant. SIC² sends the water levels to Matlab used by the MPC-MHE strategy to compute optimal control actions, which are sent back to and applied in SIC². To do so, in an online algorithm, MHE estimates immeasurable states and disturbances (water flows) every 2 minutes, while data from SIC² is received every 2 minutes to detect extreme events. Control actions determined by the MPC are applied every 2 hours to avoid excessive actuator usage. The resulting MPC solution is sent to the real system for managers' use, and the process is repeated at each time step.

In summary, the system collects data, filters it for analysis, uses a hydraulic model with a DT to estimate unknown flows, and employs MPC-MHE to determine optimal control actions, repeating the process at regular intervals. The advantages of this control architecture are twofold: first, Digital Twin-based estimation operates with real-world data, which allows for a more accurate and precise representation of the actual system's state, e.g., water levels. It is an extension of the first contribution proposed in (Duviella and Hadid, 2019). Second, the architecture provides the flexibility to apply different control strategies, e.g., MPC and LQR, allowing for a comprehensive

exploration of control methods tailored to the specific needs and conditions of the system.

DT operation

Once the filtered data (water levels and discharges) is available, the DT can be used to reproduce the real system dynamics. The levels and controls are sent to the hydraulic devices considered in the DT during a period of time. By defining an initial condition, the water volume can be computed as

$$\Delta V(k_s) = \Delta z(k_s) \cdot S_{canal}, \quad (5)$$

where S_{canal} is the area of the canal that can be simply computed as $l_{canal} \times w_{canal}$, where l_{canal} and w_{canal} are its length and width, respectively. Also, $\Delta z(k_s) = z_{canal}(k_s) - \hat{z}_{canal}(k_s)$, where $z_{canal}(k_s)$ is the measured level in canal and $\hat{z}_{canal}(k_s)$ is the estimated level comes from the hydraulic software. The difference of volume $\Delta V(k_s)$ is averaged on a time window ΔT and brings up $\mu_{\Delta V}^{\Delta T}$. Finally, the discharge difference between two consecutive time periods is given by

$$\Delta Q = \frac{\mu_{\Delta V}^{\Delta T+1} - \mu_{\Delta V}^{\Delta T}}{\Delta T}, \quad (6)$$

where the values correspond to the unknown canal inputs. Thus, for a specific period, the unknown flows can be easily defined. These values are constant during ΔT . Once the unknown inputs are estimated, the past scenarios can be replayed as in [Duvieilla and Hadid \(2019\)](#).

MPC-MHE interaction

An MPC-MHE is designed for (1) to compute the set of optimal control set points. As two tidal situations occur in practice, updated tidal information is provided by an external source at regular time instants. Then, an MPC is designed for each tidal mode, and the appropriate control action is applied at every time step of the simulation. It is interesting to note that the same MHE can be used for both tidal periods since it only determines state estimates according to the given input-output data. The whole design is carried out in [Segovia et al. \(2019\)](#) and extended in [Guekam et al. \(2021\)](#) by taking into account that N_r reaches introduce different delays $\{n_1, n_2, \dots, n_{N_r}\}$, where n_r is the

delay (in samples) for the r^{th} reach and $n = \max(n_r)$, $r \in \{1, 2, \dots, N_r\}$.

A set of operational objectives can be achieved by optimizing the value of a multi-objective cost function, where each term represents a different objective and is assigned a certain weight. Consider the following multi-objective function:

$$J = \sum_{k=1}^{N_p} \sum_{r=0}^{N_r} \ell_k^y + \ell_k^\alpha + \ell_k^{g,p} + \ell_k^{\Delta u}, \quad (7)$$

where N_r refers to the total number of reaches and N_p is the prediction horizon. Each of the objectives in (7) is described below:

- Keep water levels close to the set points:

$$\ell^y(k) = (y(k) - y_{NNL})^T W_y (y(k) - y_{NNL}), \quad (8)$$

where y_{NNL} is the NNL vector and W_y represents the weighting matrix.

- Minimize relaxation of navigability condition so that water levels stay outside the navigation bounds for a minimal amount of time:

$$\ell^\alpha(k) = \alpha(k)^T W_\alpha \alpha(k), \quad (9)$$

where $\alpha(k)$ is the relaxation term (optimization variable) and W_α is the weighting matrix.

- Minimize the operational cost of gates and pumping stations:

$$\ell^{g,p}(k) = u(k)^T W_{g,p} u(k), \quad (10)$$

where $W_{g,p}$ is a weighting matrix whose entries are adjusted according to the type of the actuator, i.e., W_g and W_p for gates and pumps, respectively. However, the priority is set on minimizing costs by reducing pumping, so the weight assigned to W_p is much larger than W_g .

- Minimize variations of control action set points:

$$\ell^{\Delta u}(k) = \Delta u(k)^T W_{\Delta u} \Delta u(k), \quad (11)$$

where $\Delta u(k) = u(k) - u(k-1)$, and $W_{\Delta u}$ is the weighting matrix. This weight is assigned a larger value than W_g , since the priority to have a smoother control ($W_{\Delta u}$) is higher than that of the operational cost of opening/closing the gates.

In this paper, as a simple way to convert the multi-objective problem into a single objective problem, a scalarization approach has been applied to minimize the weighted sum of all the objectives.

MPC formulation

The multi-objective cost function (7) is minimized by solving the optimization-based control problem along the prediction horizon. A receding-horizon strategy is followed, whereby the first value of the sequence of optimal control inputs, i.e., the MPC solution, is applied to the system, and the rest are discarded. The MPC is then solved at the next time instant by utilizing updated information (Camacho and Alba, 2013). Considering that the gates are only used in low tide mode, the low tide optimal vector of control actions is given by the solution of the following finite-time horizon optimization problem:

$$\min_{\{\mathbf{u}_{i|k}\}_{i=k}^{k+N_p-1}} \sum_{i=k}^{k+N_p-1} \left(\ell_{i|k}^y + \ell_{i|k}^\alpha + \ell_{i|k}^{g,p} + \ell_{i|k}^{\Delta u} \right) \quad (12a)$$

subject to:

$$\mathbf{x}_{i+1|k} = \mathbf{A}\mathbf{x}_{i|k} + \mathbf{B}_u^g \mathbf{u}_{i|k}^g + \mathbf{B}_u^p \mathbf{u}_{i|k}^p + \mathbf{B}_{un}^g \mathbf{u}_{i-n|k}^g + \mathbf{B}_{un}^p \mathbf{u}_{i-n|k}^p + \mathbf{B}_d \mathbf{d}_{i|k} + \mathbf{B}_{dn} \mathbf{d}_{i-n|k}, \quad (12b)$$

$$i \in \{k, \dots, k+N_p-1\}$$

$$\mathbf{y}_{i|k} = \mathbf{C}\mathbf{x}_{i|k} + \mathbf{D}_u^g \mathbf{u}_{i|k}^g + \mathbf{D}_u^p \mathbf{u}_{i|k}^p + \mathbf{D}_{un}^g \mathbf{u}_{i-n|k}^g + \mathbf{D}_{un}^p \mathbf{u}_{i-n|k}^p + \mathbf{D}_d \mathbf{d}_{i|k} + \mathbf{D}_{dn} \mathbf{d}_{i-n|k}, \quad (12c)$$

$$i \in \{k, \dots, k + N_p - 1\}$$

$$\underline{\mathbf{u}}^g \leq \mathbf{u}_{i|k}^g \leq \bar{\mathbf{u}}^g, \quad i \in \{k, \dots, k + N_p - 1\}, \quad (12d)$$

$$\underline{\mathbf{u}}^p \leq \mathbf{u}_{i|k}^p \leq \bar{\mathbf{u}}^p, \quad i \in \{k, \dots, k + N_p - 1\}, \quad (12e)$$

$$\underline{\mathbf{y}} - \alpha_{i|k} \leq \mathbf{y}_{i|k} \leq \bar{\mathbf{y}} + \alpha_{i|k}, \quad i \in \{k, \dots, k + N_p - 1\}, \quad (12f)$$

$$\alpha_{i|k} \geq \mathbf{0}, \quad i \in \{k, \dots, k + N_p - 1\}, \quad (12g)$$

$$\mathbf{d}_{j|k} = \hat{\mathbf{d}}_j^{MHE}, \quad j \in \{k - n, \dots, k\}, \quad (12h)$$

$$\mathbf{u}_{l|k}^g = \mathbf{u}_l^{MPC(g)}, \quad l \in \{k - n, \dots, k - 1\}, \quad (12i)$$

$$\mathbf{u}_{l|k}^p = \mathbf{u}_l^{MPC(p)}, \quad l \in \{k - n, \dots, k - 1\}, \quad (12j)$$

where $\mathbf{x}_k \in \mathbb{R}^{n_x}$ are the states, $\mathbf{y}_k \in \mathbb{R}^{n_y}$ are the water levels, $\mathbf{u}_k^g \in \mathbb{R}^{n_{ug}}$ and $\mathbf{u}_k^p \in \mathbb{R}^{n_{up}}$ are the total gate and pumping control actions, respectively, $\mathbf{d}_k \in \mathbb{R}^{n_d}$ are the disturbances, and $\alpha_k \in \mathbb{R}^{n_y}$ is the relaxation variable. Moreover, N_p denotes the prediction horizon, $\bar{\mathbf{u}}^g, \underline{\mathbf{u}}^g, \bar{\mathbf{u}}^p, \underline{\mathbf{u}}^p, \bar{\mathbf{y}}, \underline{\mathbf{y}}$, represent the upper and lower bounds on the gate actions, pumping actions and navigation interval bounds, respectively. Matrices $A, B_u, B_{u_n}, B_d, B_{d_n}$ are time-invariant matrices of appropriate dimensions, and can be built using the matrices of each individual reach, given by (3) and (4).

Solution of (12a) is given by $\mathbf{u}^{g*}(k) = \{\mathbf{u}_{i|k}^g\}_{i \in \mathbb{Z}_{[k, k+N_p-1]}}$ and $\mathbf{u}^{p*}(k) = \{\mathbf{u}_{i|k}^p\}_{i \in \mathbb{Z}_{[k, k+N_p-1]}}$. However, only $\mathbf{u}_{k|k}^g \in \mathbb{R}_{\geq 0}$ and $\mathbf{u}_{k|k}^p \in \mathbb{R}_{\geq 0}$ is applied; $\mathbf{u}_k^{MPC(g)} \triangleq \mathbf{u}_{k|k}^g$ and $\mathbf{u}_k^{MPC(p)} \triangleq \mathbf{u}_{k|k}^p$. On the other hand, the states $\hat{\mathbf{x}}_j^{MHE}$ and the disturbances $\hat{\mathbf{d}}_j^{MHE}$ are estimated as the solution of the MHE. Since gates are not allowed to be used in high tide mode, the same MPC can be solved for high tide conditions, but by removing the terms associated with gates.

MHE formulation

The most popular stage cost is quadratic since it can be linked to a Gaussian distribution of disturbances. In MHE, the stage cost chooses the disturbances that have a higher possibility over others. Thus, only a finite number of recent measurements are included, to keep the problem bounded in size, and is shifted in time to estimate the states in a gradual manner to exploit the most recent information (Allan and Rawlings, 2019).

The solution of the MHE, which takes the following form, yields the state estimates $\hat{\mathbf{x}}_j^{MHE}$ (which are provided to the MPC):

$$\min_{\substack{\{\hat{\mathbf{x}}_{i|k}\}_{i=k-N_e+1}^{k+1} \\ \{\hat{\mathbf{d}}_{i|k}\}_{i=k-N_e+1}^k}} \mathbf{w}_{k-N_e+1|k}^\top \mathbf{P}^{-1} \mathbf{w}_{k-N_e+1|k} + \sum_{i=k-N_e+1}^k \left(\mathbf{w}_{i|k}^\top \mathbf{Q}^{-1} \mathbf{w}_{i|k} + \mathbf{v}_{i|k}^\top \mathbf{R}^{-1} \mathbf{v}_{i|k} \right) \quad (13a)$$

subject to:

$$\mathbf{w}_{k-N_e+1|k} = \hat{\mathbf{x}}_{k-N_e+1|k} - \mathbf{x}_{k-N_e+1}, \quad (13b)$$

$$\mathbf{w}_{i|k} = \hat{\mathbf{x}}_{i+1|k} - \left(\mathbf{A}\hat{\mathbf{x}}_{i|k} + \mathbf{B}_u^g \mathbf{u}_{i|k}^g + \mathbf{B}_u^p \mathbf{u}_{i|k}^p + \mathbf{B}_{un}^g \mathbf{u}_{i-n|k}^g + \mathbf{B}_{un}^p \mathbf{u}_{i-n|k}^p + \mathbf{B}_d \hat{\mathbf{d}}_{i|k} + \mathbf{B}_{dn} \hat{\mathbf{d}}_{i-n|k} \right), \quad (13c)$$

$$i \in \{k - N + 1, \dots, k\}, \quad (13d)$$

$$\mathbf{v}_{i|k} = \mathbf{y}_{i|k} - \left(\mathbf{C}\hat{\mathbf{x}}_{i|k} + \mathbf{D}_u^g \mathbf{u}_{i|k}^g + \mathbf{D}_u^p \mathbf{u}_{i|k}^p + \mathbf{D}_{un}^g \mathbf{u}_{i-n|k}^g + \mathbf{D}_{un}^p \mathbf{u}_{i-n|k}^p + \mathbf{D}_d \hat{\mathbf{d}}_{i|k} + \mathbf{D}_{dn} \hat{\mathbf{d}}_{i-n|k} \right), \quad (13e)$$

$$i \in \{k - N + 1, \dots, k\}, \quad (13f)$$

$$\mathbf{y}_{i|k} = \mathbf{y}_i, \quad i \in \{k - N + 1, \dots, k\}, \quad (13g)$$

$$\hat{\mathbf{d}}_{i|k} \geq \mathbf{0}, \quad i \in \{k - N + 1, \dots, k\}, \quad (13h)$$

$$\underline{\mathbf{x}} \leq \hat{\mathbf{x}}_{j|k} \leq \bar{\mathbf{x}}, \quad j \in \{k - N + 1, \dots, k + 1\}, \quad (13i)$$

$$\hat{\mathbf{x}}_{l|k} = \hat{\mathbf{x}}_l^{MHE}, \quad l \in \{k - N - n + 1, \dots, k - N\}, \quad (13j)$$

$$\hat{\mathbf{d}}_{l|k} = \hat{\mathbf{d}}_l^{MHE}, \quad l \in \{k - N - n + 1, \dots, k - N\}, \quad (13k)$$

$$\mathbf{u}_{m|k}^g = \mathbf{u}_m^{MPC(g)}, \quad m \in \{k - N - n + 1, \dots, k\}, \quad (13l)$$

$$\mathbf{u}_{m|k}^p = \mathbf{u}_m^{MPC(p)}, \quad m \in \{k - N - n + 1, \dots, k\}, \quad (13m)$$

where N_e is the length of the window, \mathbf{P}^{-1} , \mathbf{Q}^{-1} and \mathbf{R}^{-1} are the weighting matrices, \mathbf{x}_{k-N+1} is the most likely initial state and \mathbf{y}_i are the measured water levels. By solving problem (13a) the optimal sequences $\{\hat{\mathbf{x}}_{i|k}\}_{i=k-N_e+1}^{k+1}$ and $\{\hat{\mathbf{d}}_{i|k}\}_{i=k-N+1}^k$ are determined, and due to the MHE principle, only one value in the sequence is kept, and the rest are discarded. In MHE, this value corresponds to the last component of the sequences, thus, $\hat{\mathbf{x}}_k^{MHE} \triangleq \hat{\mathbf{x}}_{k+1|k}$ and $\hat{\mathbf{d}}_k^{MHE} \triangleq \hat{\mathbf{d}}_{k|k}$.

Selecting appropriate weights in the MPC and MHE is invariably a challenging task, as the weights need to be carefully chosen to prevent infeasibility (Garrett and Best, 2013) while also fulfilling the desired objectives. While exist different approaches to tune the weighting parameters (Garriga and Soroush, 2010), the approach selected in this work consists of running a number of trial-and-error simulations with different combinations of values (Branch, 2011). One of the main issues linked to this method is that there is no way to evaluate the weights, as this evaluation requires another weighting vector, and this is why the tuning will be applied through trial-and-error (Mohammadi et al., 2018). This approach has been widely employed in the literature (Clemmens and Wahlin, 2004; Suicmez and Kutay, 2014; Bekkar and Ferkous, 2022).

THE CALAIS CANAL

The Calais canal is located in the north of France, in a territory called the Wateringues. This region is located below the sea level, and spreads over a triangle area of 100000 hectares, with a network length of approximately 1500 km (see Figure 1). The network is equipped with different actuators such as gates for the sea and water pumps (Ranjbar et al., 2022). The main reach is the Calais canal which can be divided into three sectors, each of them supplied by secondary canals named Audruicq canal, Ardres canal and Guines canal (see Figure 2) that the discharges of those are currently not controlled. At the upstream end of the canal, the Hennuin lock is used for navigation purposes; at the downstream end, there are sea outlet gates with two pumps located in Calais, each of them has a capacity of $4m^3/s$, and two others in Batellerie (close to Calais), each with a capacity of $2m^3/s$. In this study, the pumping station in Batellerie is ON (pump type Jeumont-Schneider 90PHO200). Two level sensors make it possible to measure the water levels at Calais and Attaques (Z_{attaq} and Z_{calais}) and thus provide measurements for control purposes.

The total length of the canal is $L = 26.72km$ with an average width of $W = 20m$ and depth of $D = 2.2m$. The canal is also equipped with a total of 18 pumping stations situated along the reach, which are used by farmers according to their needs and experience. Moreover, when a pumping station is OFF, there is no discharge; conversely, when it is on, the average discharge is a known

quantity, as displayed in Figure 2 in brackets. For instance, PS_{Mower} supplies $0.35m^3/s$ when such pump is ON. When all pumping stations are ON, the combined flow is equal to $8.46m^3/s$. It should be mentioned that the estimation of maximum flows of the three secondary canals are respectively $Q_{Audruicq} = 3m^3/s$, $Q_{Ardres} = 1m^3/s$ and $Q_{Guines} = 0.2m^3/s$ denoting that there is a maximum input flow equal to $13.06m^3/s$ through all the pumping stations and the residual amount of $0.4m^3/s$ is the runoff generated from surface water. These pumping stations cannot be used for the objective of water level regulation. While the sea pumps located in Calais and Batellerie act as the system's inputs, the pumping from the 18 pumping stations by the farmers are the disturbances applied to the system.

A semidiurnal tidal pattern of two low and two high tides per day (in other words, each tide with an approximate duration of six hours) is considered based on the canal location. The excess water is periodically discharged to the sea, thanks to the gates located in Calais where the total flow supplied by these gates is bounded between $0m^3/s$ and $12.50m^3/s$ or $15m^3/s$ depending on the type of tides, e.g. neap and spring tides (*see* Figure 3). Spring tides cause regular high tides and low tides to be much higher than usual, and neap tides cause the regular high tides and low tides to become much lower than usual. This figure focuses on the manager's objectives regarding the gate opening and discharge through the real samples shown with the stars.

The water level in the canal must be regulated around the NNL . An interval around the NNL is considered for water level control, which provides more flexibility. This interval corresponds to $HNL = NNL + 13cm$ and $LNL = NNL - 50cm$, with *High Navigation Level (HNL)* and *Low Navigation Level (LNL)*. In other words, during high tide, the water level may rise close to the HNL , and then recede to the LNL with the next low tide, when the outlet gates can be operated again. Hence, the water level could oscillate around NNL , limiting the use of pumps. Another extreme high limit is introduced as *Flooding Limit*, $FL = NNL + 33cm$. It is imperative to keep the level of the canal below this value.

EXPERT RULES-BASED MANAGEMENT

The management of the Calais canal is extremely complex and involves a large number of

stakeholders, such as technical professionals. It aims to fulfill the management objectives by determining the conditions to operate the hydraulic structures, i.e., the gates and the pumps in Calais and Battellerie as in Figure 2. The Calais canal managers have acquired several decades of experience in terms of its management, and have defined protocols to coordinate the actions of all stakeholders in the general interest. Moreover, a Supervisory Control And Data Acquisition (SCADA) has been implemented to monitor, gather, and process real-time data from the Calais canal. This allows for direct communication with sensors and actuators through a human-machine interface (HMI) software, and also to record data and regulate the canal according to the management protocols. These are synthesized as the expert rules that are visually represented in Figure 4 (Duviella and Hadid, 2019). In this diagram, the initial condition determines whether the Calais gates can be opened according to the tidal conditions. High tide can be assumed when Z_{calais} is less than Z_{sea} , where Z_{calais} is the level in Calais and Z_{sea} represents the sea level. During high tide, no pumping action occurs if Z_{attaq} is below the NNL and the rate of hydrograph increase (i.e., how quickly the discharge rises in response to factors like rainfall), denoted as Z_{attaq}^{-1} , is less than $3cm/h$. Activation of the pumps in Calais is contingent on Z_{attaq} exceeding the NNL or if Z_{attaq}^{-1} exceeds $3cm/h$. Furthermore, the Battellerie pumps are activated when Z_{attaq}^{-1} exceeds $7cm/h$, which represents a substantial inflow of water into the Calais canal.

During low tide, the accumulated rainfall over 12 hours and 24 hours are considered, which are denoted as p_{12h} and p_{24h} , respectively. If p_{24h} is less than $10mm$, this indicates a non-rainy scenario, and the Calais gates operate under normal conditions. In rainy situations, the Calais gates are opened excessively if p_{12h} is less than $10mm$ or if the pumps were inactive during the previous tide. However, in cases of heavy rainfall when p_{12h} exceeds $10mm$ and the pumps were in operation during the previous tide, the Calais gates are fully opened. In the event of overflow, the Calais gates are immediately opened to their maximum capacity, and the Battellerie pumps are activated. Real data that is processed originates from the SCADA system. The hydraulic devices operate automatically, guided by expert rules, which in turn influence the observed water levels (refer to Figure 5, the last subplot). By utilizing this dataset, it becomes possible to either bypass or

replace the control system based on expert rules with a custom-designed and implemented one. As a result, the performance of these new control algorithms will be evaluated by directly comparing them to the control systems established using expert rules. The proposed architecture based on the DT allows the determination of unknown inputs from secondary canals, rain, and uncontrolled pumping stations. It is therefore possible to replay the scenario using a new control approach as the MPC-MHE in Section 3. Finally, the operations on the hydraulic devices, determined by the expert rules, are improved by those of the MPC.

SIMULATION AND RESULTS

The proposed approach is applied to the case study, the Calais canal. To model this canal, the hydraulic software SIC² is used to generate an accurate model of the canal based on the numerical solution of the 1D Saint-Venant equations, which describes the dynamic behavior of open-channel systems with great accuracy (Malaterre et al., 2015). In SIC², the effect of certain real disturbances including the farmers' pumping, the water transfers caused by the movement of boats through the canal, and the secondary canals' discharges are studied on the Calais canal model. Data acquired in November 2019 is used in this study, a period during which heavy rainfall is the primary factor affecting farmers' activities. Due to this rainfall, the possibility of flooding leads farmers to pump excess water from their fields. In severe situations, their actions may become less predictable. Thus, in this scenario, the farmers' activity is affected by rainy conditions. However, during spring and summer, their activities can be adjusted based on seasonal components, e.g., growing period of crops (Arandia et al., 2016).

The linear discrete-time equations with delays (3),(4) are considered in both MPC and MHE. For model discretization, two sampling times have been selected as described in section 3. Moreover, both prediction horizon N_p and estimation window size N_e are considered to be 12 hours to include complete high and low tide periods, each of them with an average duration equal to 6 hours. Based on the runoff data for the given period and considering the pump dynamics, a duration of 6 hours is deemed suitable for capturing the average incoming flows in this study. Simulation of the real conditions on the system built in SIC² allows obtaining results for a 3-day period using the CPLEX

12.10.0 optimization package, Matlab R2019b (64 bits), and YALMIP (Lofberg, 2004).

The cost function weights in Equation (7) are defined in a similar manner for both low tide and high tide modes, as detailed below. Depending on the priority of each objective, these weights in MPC can be customized to assign greater importance to specific objectives (Karimi Pour et al., 2022). They are carefully adjusted through an iterative tuning process, as described in Section 3. The following weights are selected to minimize the most critical objective first, ensure appropriate water levels within the navigation rectangle, minimize economic costs, maintain smooth control actions, and penalize relaxation parameters simultaneously: $W_y = 1$, $W_\alpha = 10$, $W_g = 1$, $W_p = 1000$, $W_{\Delta u} = 10$.

Figure 5 shows the managers' control of the discharges and levels in the Calais canal and the estimation of unknown inputs/outputs achieved from DT. The colored periods correspond to high-tide periods, while the non-colored areas are the low-tide periods. The first subplot shows the estimated water flow in all three sections of the canal (see Figure 2), where the upper dotted lines are the discharge in section 1 (upstream of the canal, Q_1) with a maximum flow of around $2.5 \text{ m}^3/\text{s}$. The solid line is the one of section 2 (in the middle of the canal, Q_2) which goes up to $1 \text{ m}^3/\text{s}$ after two days. The lower dotted line is used for section 3 (Q_3), which has the lowest discharge during the three days. Note that Q_4 shows the outlet discharges in Figure 2. All in all, this subplot demonstrates the importance of the application of the DT to control the Calais canal, since the above-mentioned discharges could not be considered precisely without it. The second subplot represents the separated measured discharges of the gates (Q_g) in the upper dotted line and the pumps (Q_p) in the solid line. It can be seen that managers' rules lead to opening the gates frequently to release water with outflows ranging from $3 \text{ m}^3/\text{s}$ to $15 \text{ m}^3/\text{s}$. Moreover, the pumps are employed occasionally, with a discharge of around $4 \text{ m}^3/\text{s}$ (the average discharge of one pump in Calais). This substantial discharge and the requirement for pumping result from the application of the expert-rules based management in the real scenario. The third subplot depicts the sea level (sin wave) and the level in Calais (solid line). Subplot four displays the estimated discharge of all three secondary canals, where the upper dotted line stands for Audruicq, the solid line corresponds

to Ardres, and the lower dotted line is for Guines. The increase of the discharge from secondary canals from November, 1st at 16:00 to November 3rd at 12:00 is due to the rain. The fifth subplot shows the water level in Calais (solid sine wave) along with its estimation done by the DT, *i.e.* SIC² (dashed sine wave), with two upper bounds, the upper solid line is the *HNL* in the canal which is set to $NNL + 15cm$, *i.e.* $HNL = 2.35m$ and the upper dashed-dot line is the maximum allowable level in Calais, *i.e.* $NNL + 33cm, FL = 2.53m$. This subplot acknowledges that the difference between the real level, obtained through the expert rules-based management, and the level provided by SIC² is not large, once again emphasizing the practical significance of the DT.

Figure 6 shows that after estimating the unknown discharges, the error between the estimated water level by the DT and the real water level is not large, with the following statistical measures highlighting the reliability and accuracy of the estimation: the maximum error is $12.38cm$, the mean is $2.07cm$, the standard deviation is $3.58cm$, and the median is $1.19cm$.

Figure 7 shows the control actions of the gates and pumps using two different approaches: one based on expert rules and the proposed control architecture: the first subplot depicts the discharge that managers decide for the gates (with a maximum of $18m^3/s$), and the MPC solution for the so, with a lower discharge. Managers open the gate as soon as the canal level becomes higher than the sea level. However, MPC switches from high tide to low tide only based on fixed high/low tide period assumptions, here 6 hours. After the control implementation, there is less discharge supplied by the gates, with a maximum of $12.72m^3/s$ and a minimum of $0.9m^3/s$ during this period, demonstrating the effectiveness of the control architecture compared to the expert rules-based managing in order to minimize the operational cost of gates according to the Equation (10). Also, the gates are used smoothly (*i.e.*, fluctuations are small) as the weight assigned to this objective is large ($W_g = 10$) during low-tide periods (white background). This plot reveals that the increase in how many times the gates are controlled (opened/closed) from 3 times by managers to 6 times after applying the control approach is a tangible manifestation of MPC's reactive control action in dynamic and unpredictable environments for maintaining the desired process performance. Another weight tuning could adjust this issue, providing less number of controls for the gate, and

inducing more fluctuation of the level. However, this depends on the management objectives and their relative importance.

The second subplot emphasizes that the pumps are not activated in the MPC solution, which aligns well with the real application, in which it is desirable to minimize/avoid using the pumps and to switch their activation states due to associated maintenance problems and economic reasons. As long as the level is kept within the navigation rectangle, it is decided not to operate the pumps. This control action prohibits the 14.63 hours of pumping in reality, operated by expert rules-based management. Since an hour of pumping requires 250 kWh energy, a total amount of 3658.25 kWh has been economized, with an equivalent cost around €763 . This represents a substantial advantage compared to the expert rules-based management, in which the Batellerie pumps were activated with a discharge rate of $2m^3/s$ to increase the discharge capacity of the sea outlet pumps while raining. This is the main and most important objective of the control architecture in this real scenario (the weight assigned to this objective in the cost function is the largest, i.e., $W_p = 1000$).

The third and fourth subplots display the water levels in Calais and Attaque oscillating around the *NNL* and inside the navigation boundaries. It can be seen that the real water level in Attaque oscillates a lot during the period of simulation. Applying the proposed control architecture, the oscillation is not large and is bounded within *HNL* and *LNL*. The water level rises up to the *HNL* level only once during the simulation time, which is acceptable from the operational viewpoint. Moreover, since the level is very close to the *NNL* during the first day, due to the initialization of MPC, the water level could go up close to the *HNL*.

CONCLUSION

This paper focused on implementing an MPC-MHE considering a multi-objective control problem using a real database of a water canal, and the performance of this approach is evaluated. A Digital Twin (DT) designed as a Matlab-SIC² architecture was used to reproduce the dynamics of canals and to estimate the unknown inputs/outputs. Based on this consolidated database, the control algorithms can be tested. Data for the Calais canal corresponding to a period of three days was assigned to illustrate all the proposed steps. An MPC–MHE approach was designed considering

two different modes, one for high tide and another for low tide. The control strategy aims to fulfill the management objectives by avoiding the use of pumps. The simulation results acknowledge that the whole multi-objective control problem satisfies the managers' objectives while maintaining the water levels inside the navigation interval, thus keeping the effects of severe weather periods under control. This methodology demonstrates superior results in both economic and functional aspects compared to the application of expert rules-based management.

The next step, in the context of real application, is to make all the tools developed available to managers so that they can study larger periods of data. A transcription work in Python has already been started (Pour et al., 2022) that can be integrated with the digital twin and other software engineering solutions. In the framework of scientific research, the challenge would be to predict unknown water inflows or outflows using unknown input observers (Guan and Saif, 1991) or machine learning approaches (Hadid et al., 2020), and couple this information with the control algorithms.

DATA AVAILABILITY STATEMENT

Some or all data used during the study were provided by a third party; the IIW (Institution Intercommunale des Watingues). Direct requests for these materials may be made to the provider.

ACKNOWLEDGEMENT

This work has been supported by the Regional Council of Hauts-de-France and the IIW (Institution Intercommunale des Watingues) and has received funding from the H2020 ADG-ERC OCONTSOLAR Project under Grant 789051. Authors gratefully thank these institutions for their support.

References

Allan, D. A. and Rawlings, J. B. (2019). "Moving horizon estimation." *Handbook of Model Predictive Control*, Springer, 99–124.

- Arandia, E., Ba, A., Eck, B., and McKenna, S. (2016). "Tailoring seasonal time series models to forecast short-term water demand." *Journal of Water Resources Planning and Management*, 142(3), 04015067.
- Bartos, M. and Kerkez, B. (2021). "Pipedream: An interactive digital twin model for natural and urban drainage systems." *Environmental Modelling & Software*, 144, 105120.
- Bekkar, B. and Ferkous, K. (2022). "Design of online fuzzy tuning lqr controller applied to rotary single inverted pendulum: Experimental validation." *Arabian Journal for Science and Engineering*, 1–16.
- Branch, S. T. (2011). "Optimal design of lqr weighting matrices based on intelligent optimization methods." *International Journal of Intelligent Information Processing*, 2(1), 63–74.
- Bresch, D. (2009). "Shallow-water equations and related topics." *Handbook of differential equations: evolutionary equations*, 5, 1–104.
- Camacho, E. F. and Alba, C. B. (2013). *Model predictive control*. Springer science & business media.
- Camacho, E. F. and Bordons, C. (2007). "Nonlinear model predictive control: An introductory review." *Assessment and future directions of nonlinear model predictive control*, 1–16.
- Castelletti, A., Ficchi, A., Cominola, A., Segovia, P., Giuliani, M., Wu, W., Lucia, S., Ocampo-Martinez, C., De Schutter, B., and Maestre, J. M. (2023). "Model predictive control of water resources systems: A review and research agenda." *Annual Reviews in Control*.
- Clemmens, A., Tian, X., van Overloop, P.-J., and Litrico, X. (2017). "Integrator delay zero model for design of upstream water-level controllers." *Journal of Irrigation and Drainage Engineering*, 143(3), B4015001.
- Clemmens, A. and Wahlin, B. (2004). "Simple optimal downstream feedback canal controllers: Asce test case results." *Journal of Irrigation and Drainage Engineering*, 130(1), 35–46.

- Conejos Fuertes, P., Martínez Alzamora, F., Hervás Carot, M., and Alonso Campos, J. (2020). “Building and exploiting a digital twin for the management of drinking water distribution networks.” *Urban Water Journal*, 17(8), 704–713.
- Copp, D. A. and Hespanha, J. P. (2017). “Simultaneous nonlinear model predictive control and state estimation.” *Automatica*, 77, 143–154.
- Deshays, R., Segovia, P., and Duviella, E. (2021). “Design of a matlab hec-ras interface to test advanced control strategies on water systems.” *Water*, 13(6), 763.
- Duviella, E., Doniec, A., and Nouasse, H. (2018). “Adaptive water-resource allocation planning of inland waterways in the context of global change.” *Journal of Water Resources Planning and Management*, 144(9), 04018059.
- Duviella, E. and Hadid, B. (2019). “Simulation tool of the calais canal implementing logic control based regulation.” *IFAC-PapersOnLine*, 52(23), 23–28.
- Fele, F., Maestre, J. M., Hashemy, S. M., de la Peña, D. M., and Camacho, E. F. (2014). “Coalitional model predictive control of an irrigation canal.” *Journal of Process Control*, 24(4), 314–325.
- Garrett, N. J. and Best, M. C. (2013). “Model predictive driving simulator motion cueing algorithm with actuator-based constraints.” *Vehicle System Dynamics*, 51(8), 1151–1172.
- Garriga, J. L. and Soroush, M. (2010). “Model predictive control tuning methods: A review.” *Industrial & Engineering Chemistry Research*, 49(8), 3505–3515.
- Guan, Y. and Saif, M. (1991). “A novel approach to the design of unknown input observers.” *IEEE Transactions on Automatic Control*, 36(5), 632–635.
- Guekam, P., Segovia, P., Etienne, L., and Duviella, E. (2021). “Hierarchical model predictive control and moving horizon estimation for open-channel systems with multiple time delays.” *2021 European Control Conference (ECC)*, IEEE, 198–203.

- Hadid, B., Duviella, E., and Lecoeuche, S. (2020). “Data-driven modeling for river flood forecasting based on a piecewise linear arx system identification.” *Journal of Process Control*, 86, 44–56.
- Karimi Pour, F., Segovia, P., Duviella, E., and Puig, V. (2022). “A two-layer control architecture for operational management and hydroelectricity production maximization in inland waterways using model predictive control.” *Control Engineering Practice*, 124, 105172.
- Litrico, X. and Fromion, V. (2009). *Modeling and control of hydrosystems*. Springer Science & Business Media.
- Liu, W., Guan, G., Tian, X., Cao, Z., and Chen, X. (2023). “Exploiting a real-time self-correcting digital twin model for the middle route of the south-to-north water diversion project of china.” *Journal of Water Resources Planning and Management*, 149(7), 04023023.
- Lofberg, J. (2004). “Yalmip: A toolbox for modeling and optimization in matlab.” *2004 IEEE international conference on robotics and automation (IEEE Cat. No. 04CH37508)*, IEEE, 284–289.
- Maciejowski, J. M. (2002). *Predictive control: with constraints*. Pearson education.
- Malaterre, P.-O., Jean-Baptiste, N., and Dorée, C. (2015). “Data assimilation to improve models used for the automatic control of rivers or canals.” *Transport of Water versus Transport over Water*, Springer, 35–58.
- Mohammadi, A., Asadi, H., Mohamed, S., Nelson, K., and Nahavandi, S. (2018). “Multiobjective and interactive genetic algorithms for weight tuning of a model predictive control-based motion cueing algorithm.” *IEEE transactions on cybernetics*, 49(9), 3471–3481.
- Nasir, H. A., Cantoni, M., Li, Y., and Weyer, E. (2019). “Stochastic model predictive control based reference planning for automated open-water channels.” *IEEE Transactions on Control Systems Technology*, 29(2), 607–619.

- Pour, F. K., Duviella, E., and Segovia, P. (2022). “Development of a python tool based on model predictive control for an optimal management of the calais canal.” *IFAC-PapersOnLine*, 55(33), 1–6.
- Puig, V., Ocampo-Martínez, C., Pérez, R., Cembrano, G., Quevedo, J., and Escobet, T. (2017). *Real-time monitoring and operational control of drinking-water systems*. Springer.
- Ramos, H. M., Morani, M. C., Carravetta, A., Fecarrotta, O., Adeyeye, K., López-Jiménez, P. A., and Pérez-Sánchez, M. (2022). “New challenges towards smart systems’ efficiency by digital twin in water distribution networks.” *Water*, 14(8), 1304.
- Ranjbar, R., Duviella, E., Etienne, L., and Maestre, J.-M. (2020). “Framework for a digital twin of the canal of calais.” *Procedia Computer Science*, 178, 27–37.
- Ranjbar, R., Etienne, L., Duviella, E., and Maestre, J. M. (2022). “Sensitivity analysis of the digital twin of the canal of calais to the outlet gate modelling.” *Advances in Hydroinformatics: Models for Complex and Global Water Issues—Practices and Expectations*, Springer, 175–194.
- Schuurmans, J., Clemmens, A., Dijkstra, S., Hof, A., and Brouwer, R. (1999). “Modeling of irrigation and drainage canals for controller design.” *Journal of irrigation and drainage engineering*, 125(6), 338–344.
- Segovia, P., Blesa, J., Horváth, K., Rajaoarisoa, L., Nejari, F., Puig, V., and Duviella, E. (2018). “Modeling and fault diagnosis of flat inland navigation canals.” *Proceedings of the Institution of Mechanical Engineers, Part I: Journal of Systems and Control Engineering*, 232(6), 761–771.
- Segovia, P., Duviella, E., and Puig, V. (2020). “Multi-layer model predictive control of inland waterways with continuous and discrete actuators.” *IFAC-PapersOnLine*, 53(2), 16624–16629.
- Segovia, P., Rajaoarisoa, L., Nejari, F., Duviella, E., and Puig, V. (2019). “Model predictive control

- and moving horizon estimation for water level regulation in inland waterways.” *Journal of Process Control*, 76, 1–14.
- Shahdany, S. H., Majd, E. A., Firoozfar, A., and Maestre, J. (2016). “Improving operation of a main irrigation canal suffering from inflow fluctuation within a centralized model predictive control system: case study of roodasht canal, iran.” *Journal of Irrigation and Drainage Engineering*, 142(11), 05016007.
- Suicmez, E. C. and Kutay, A. T. (2014). “Optimal path tracking control of a quadrotor uav.” *2014 International Conference on Unmanned Aircraft Systems (ICUAS)*, IEEE, 115–125.
- Tian, X., Negenborn, R. R., van Overloop, P.-J., Maestre, J. M., Sadowska, A., and van de Giesen, N. (2017). “Efficient multi-scenario model predictive control for water resources management with ensemble streamflow forecasts.” *Advances in water resources*, 109, 58–68.
- van Overloop, P.-J., Horváth, K., and Aydin, B. E. (2014). “Model predictive control based on an integrator resonance model applied to an open water channel.” *Control Engineering Practice*, 27, 54–60.
- Velarde, P., Tian, X., Sadowska, A., and Maestre, J. (2019). “Scenario-based hierarchical and distributed mpc for water resources management with dynamical uncertainty.” *Water Resources Management*, 33(2), 677–696.
- Vermuyten, E., Meert, P., Wolfs, V., and Willems, P. (2018). “Model uncertainty reduction for real-time flood control by means of a flexible data assimilation approach and reduced conceptual models.” *Journal of Hydrology*, 564, 490–500.
- Walski, T. (2017). “Procedure for hydraulic model calibration.” *Journal (American Water Works Association)*, 109(6), 55–61.
- Zafra-Cabeza, A., Maestre, J., Ridao, M. A., Camacho, E. F., and Sánchez, L. (2011). “A hier-

archical distributed model predictive control approach to irrigation canals: A risk mitigation perspective.” *Journal of Process Control*, 21(5), 787–799.

Zekri, S., Jabeur, N., and Gharrad, H. (2022). “Smart water management using intelligent digital twins.” *Computing and Informatics*, 41(1), 135–153.

List of Figures

1	Map of the watersheds in the north of France and of the Wateringues Territory. . . .	29
2	Schematic view of the Calais canal.	30
3	Gate discharge in Calais for both the spring tide (upper line) and the neap tide (lower line).	31
4	Expert Rules regulation diagram of Duviella and Hadid (2019)	32
5	DT implementation to estimate unknown inputs in Audruicq (upper dotted line), Ardres (solid line), and Guines (lower dotted line), discharges of gates (upper dotted line) and pumps (solid line), showing real level in Calais (solid line) along with the sea level (sine wave), discharges in all three secondary canals, and the real level in Calais (solid sine wave) with that of provided from SIC ² (dashed semi-sine wave) with the <i>HNL</i> (solid upper line) and flooding threshold (dashed-dot line).	33
6	Water levels' error of estimation.	34
7	Comparison of expert rules-based management and the proposed control architecture for discharge rates through gates and pumps and the water levels in Calais and Attaque.	35

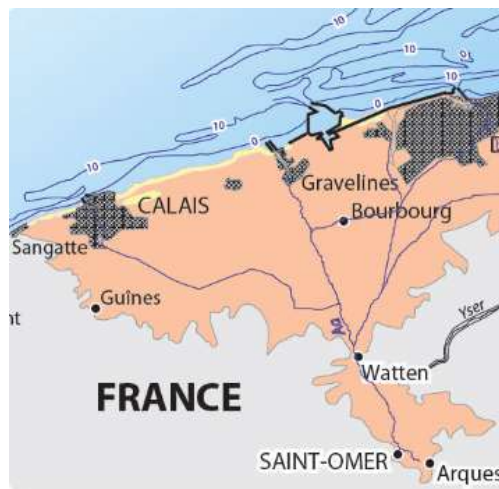


Figure 1: Map of the watersheds in the north of France and of the Wateringues Territory.

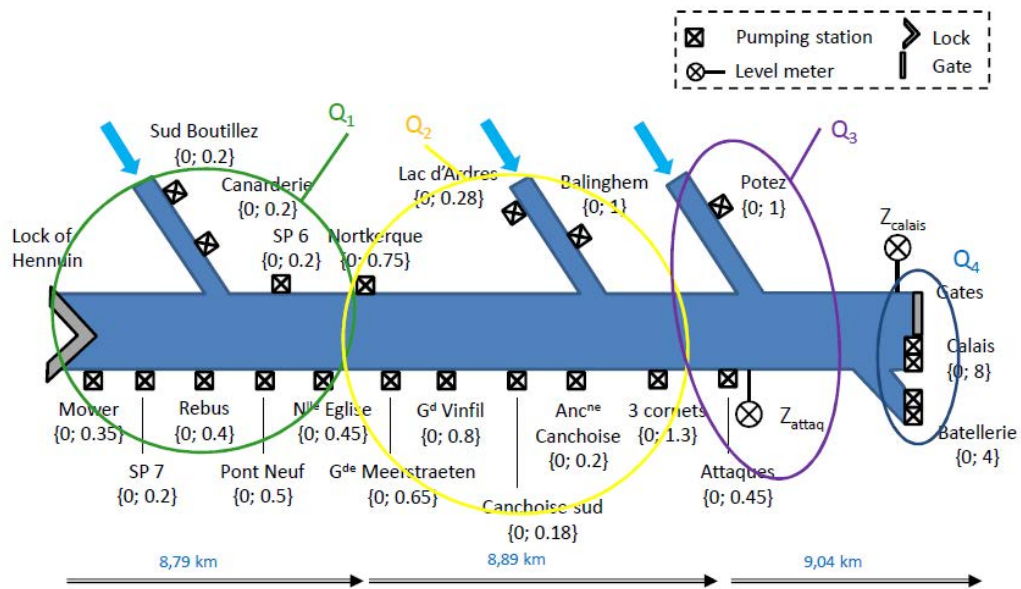


Figure 2: Schematic view of the Calais canal.

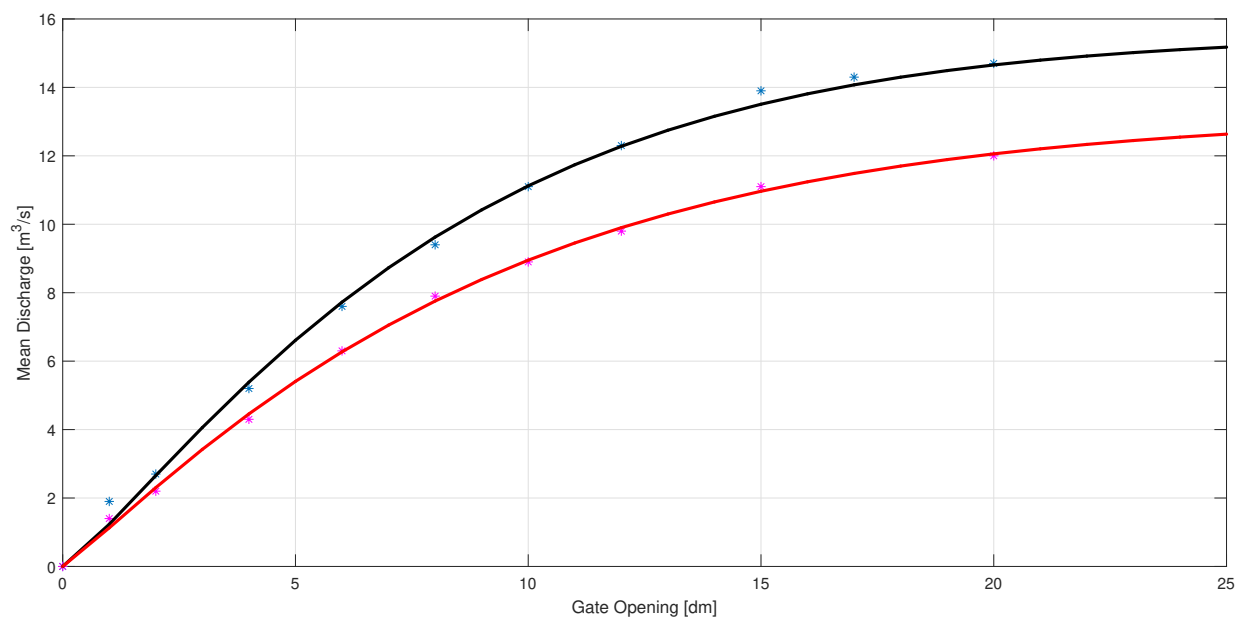


Figure 3: Gate discharge in Calais for both the spring tide (upper line) and the neap tide (lower line).

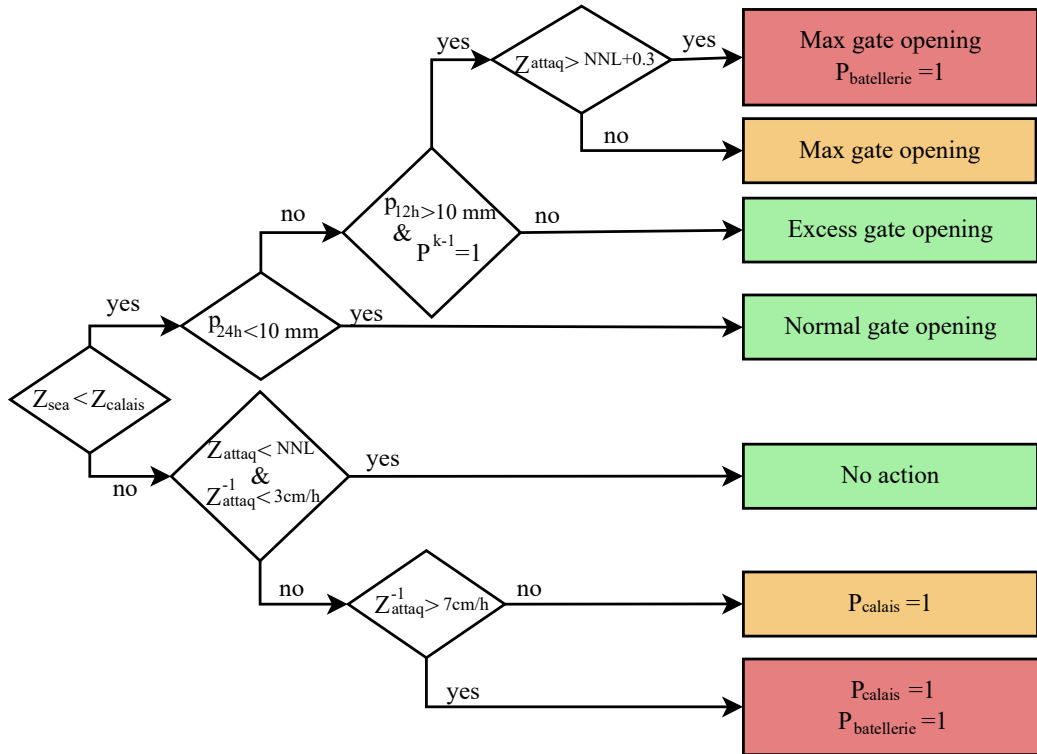


Figure 4: Expert Rules regulation diagram of **Duviella and Hadid (2019)**.

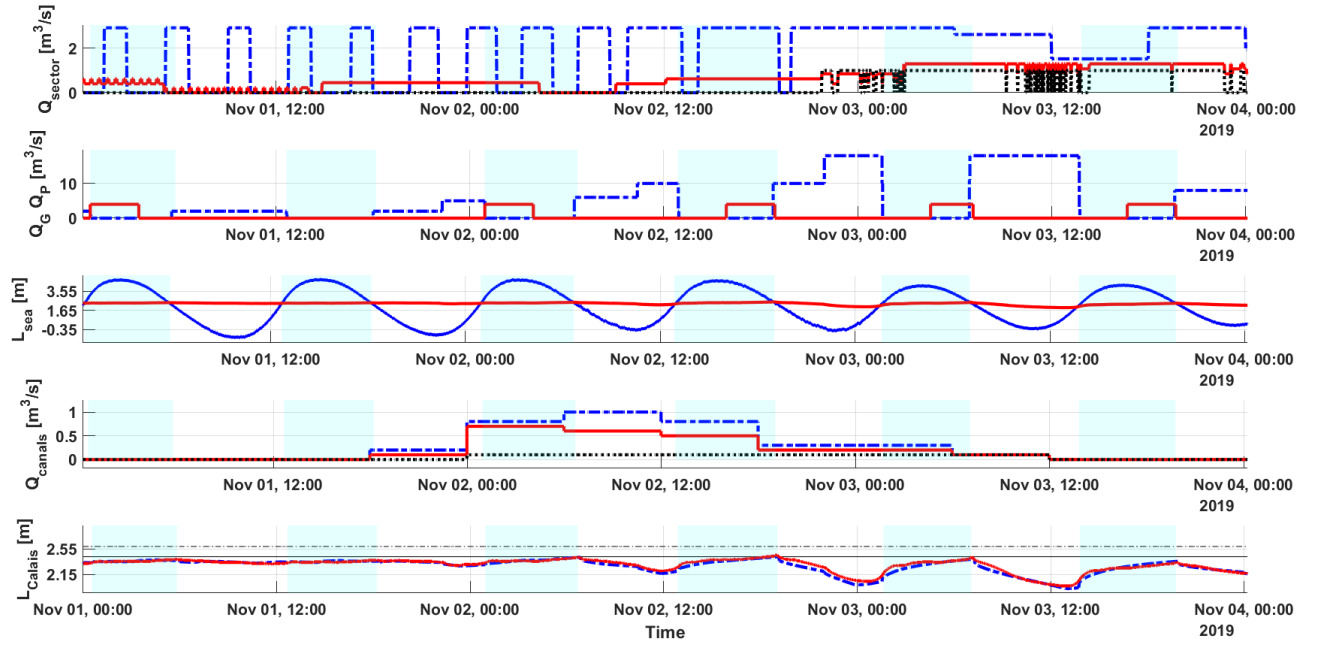


Figure 5: DT implementation to estimate unknown inputs in Audruicq (upper dotted line), Ardres (solid line), and Guines (lower dotted line), discharges of gates (upper dotted line) and pumps (solid line), showing real level in Calais (solid line) along with the sea level (sine wave), discharges in all three secondary canals, and the real level in Calais (solid sine wave) with that of provided from SIC² (dashed semi-sine wave) with the *HNL* (solid upper line) and flooding threshold (dashed-dot line).

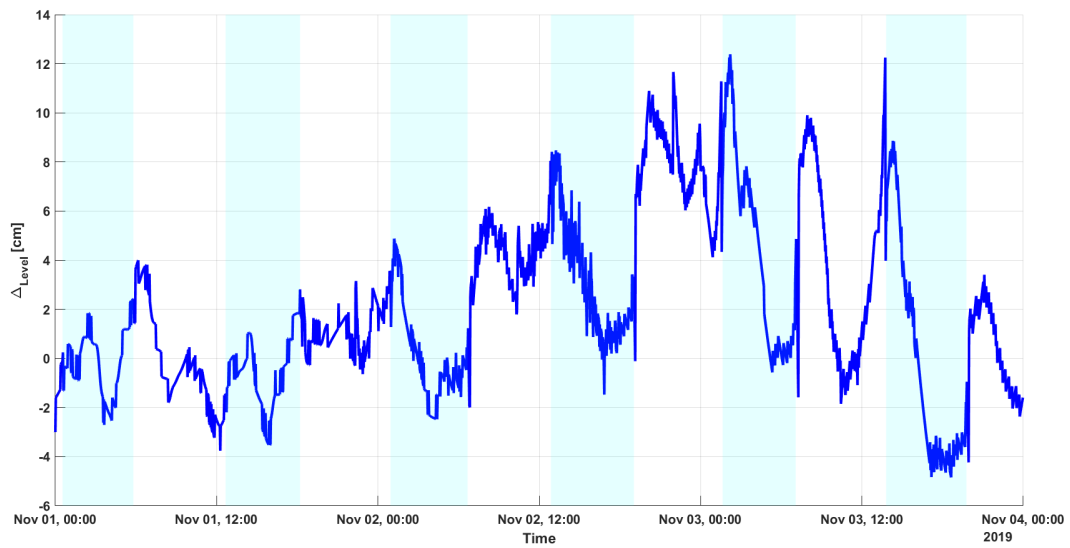


Figure 6: Water levels' error of estimation.

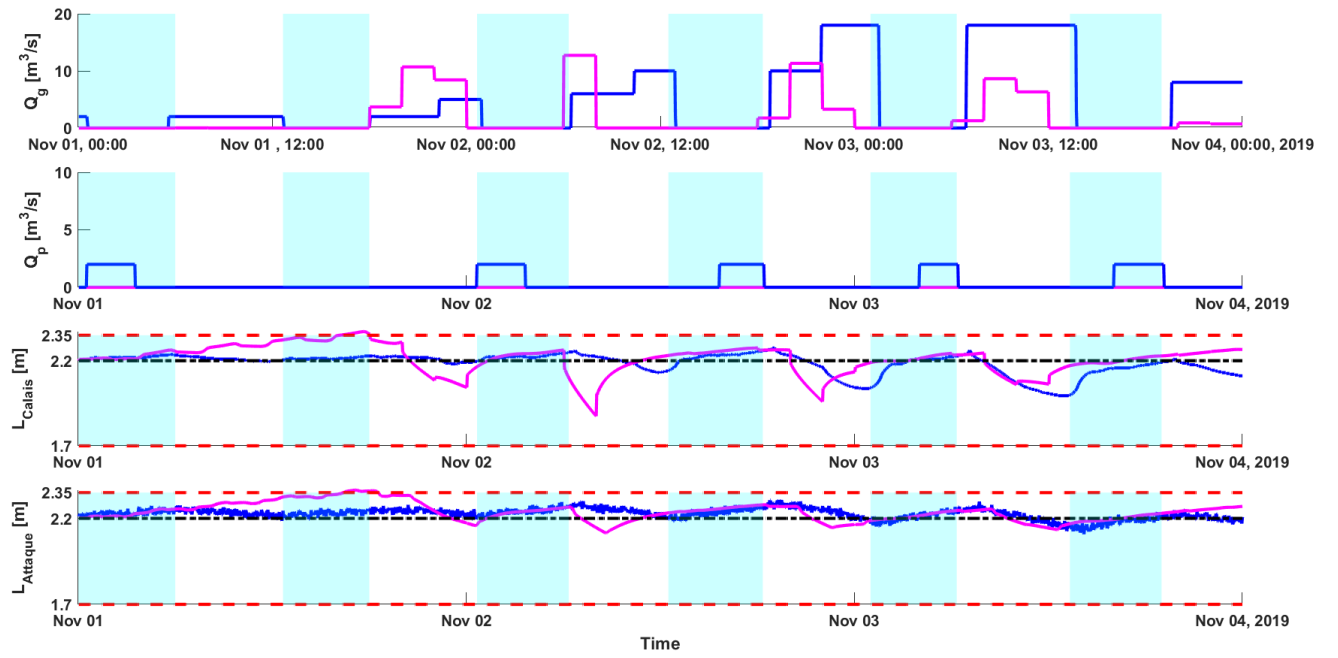


Figure 7: Comparison of expert rules-based management and the proposed control architecture for discharge rates through gates and pumps and the water levels in Calais and Attaque.